Colloids and Surfaces B: Biointerfaces 128 (2015) 191–200

Contents lists available at ScienceDirect

Colloids and Surfaces B: Biointerfaces

journal homepage: www.elsevier.com/locate/colsurfb

Mimicking bone extracellular matrix: Integrin-binding peptidomimetics enhance osteoblast-like cells adhesion, proliferation, and differentiation on titanium

Roberta Fraioli[a,b,c], Florian Rechenmacher[d], Stefanie Neubauer[d], José M. Manero[a,b], Javier Gil[a,b], Horst Kessler[d,e], Carlos Mas-Moruno[a,b,c,*]

[a] Biomaterials, Biomechanics and Tissue Engineering Group, Department of Materials Science and Metallurgical Engineering, Technical University of Catalonia (UPC), ETSEIB, Av. Diagonal 647, 08028 Barcelona, Spain
[b] Biomedical Research Networking Centre in Bioengineering, Biomaterials and Nanomedicine (CIBER-BBN), Campus Río Ebro, Edificio I+D Bloque 5, 1ª planta, C/Poeta Mariano Esquillor s/n, 50018 Zaragoza, Spain
[c] Centre for Research in NanoEngineering (CRNE) – UPC, C/Pascual i Vila 15, 08028 Barcelona, Spain
[d] Institute for Advanced Study and Center for Integrated Protein Science, Department Chemie, Technische Universität München, Lichtenbergstr. 4, 85747 Garching, Germany
[e] Chemistry Department, Faculty of Science, King Abdulaziz University, Jeddah, Saudi Arabia

ARTICLE INFO

Article history:
Received 14 October 2014
Received in revised form
27 November 2014
Accepted 24 December 2014
Available online 13 January 2015

Keywords:
Peptidomimetics
Integrins
Titanium
Functionalization
Osteointegration

ABSTRACT

Interaction between the surface of implants and biological tissues is a key aspect of biomaterials research. Apart from fulfilling the non-toxicity and structural requirements, synthetic materials are asked to direct cell response, offering engineered cues that provide specific instructions to cells. This work explores the functionalization of titanium with integrin-binding peptidomimetics as a novel and powerful strategy to improve the adhesion, proliferation and differentiation of osteoblast-like cells to implant materials. Such biomimetic strategy aims at targeting integrins $\alpha v\beta 3$ and $\alpha 5\beta 1$, which are highly expressed on osteoblasts and are essential for many fundamental functions in bone tissue development. The successful grafting of the bioactive molecules on titanium is proven by contact angle measurements, X-ray photoelectron spectroscopy and fluorescent labeling. Early attachment and spreading of cells are statistically enhanced by both peptidomimetics compared to unmodified titanium, reaching values of cell adhesion comparable to those obtained with full-length extracellular matrix proteins. Moreover, an increase in alkaline phosphatase activity, and statistically higher cell proliferation and mineralization are observed on surfaces coated with the peptidomimetics. This study shows an unprecedented biological activity for low-molecular-weight ligands on titanium, and gives striking evidence of the potential of these molecules to foster bone regeneration on implant materials.

1. Introduction

Surface modification of metallic materials is a well-established strategy to convey enhanced bioactivity to metallic implants while keeping their excellent bulk properties [1]. In this regard, commercially pure titanium (CP Ti) and Ti6Al4V, the materials of choice for most dental and orthopedic applications [2], have been subjected to surface treatments to improve their interaction with surrounding tissues, and ensure a rapid and long-lasting osteointegration of the biomaterial. In particular, the long-term stability of the implant has become a serious issue to address, as the age of patients receiving surgery is gradually decreasing, while life expectancy is ever-increasing.

A high number of surface modification methods have been described to improve the biological performance of Ti-based materials, including physical treatments, which modify the topography of the surface [3–5], chemical modifications or a combination of these approaches. All these techniques aim at creating the proper physicochemical microenvironment to elicit an optimal interaction with osteoblast (OB) and osteoprecursor cells, which is a crucial step to obtain a successful osteointegration of the implant material. In detail, the rationale for modifying the chemical nature of Ti surfaces is to obtain bioactive surfaces capable of establishing stronger

* Corresponding author at: Biomaterials, Biomechanics and Tissue Engineering Group, Department of Materials Science and Metallurgical Engineering, Technical University of Catalonia (UPC), ETSEIB, Av. Diagonal 647, 08028 Barcelona, Spain. Tel.: +34 93 401 08 14; fax: +34 93 401 67 06.
E-mail address: carles.mas.moruno@upc.edu (C. Mas-Moruno).

http://dx.doi.org/10.1016/j.colsurfb.2014.12.057
0927-7765/

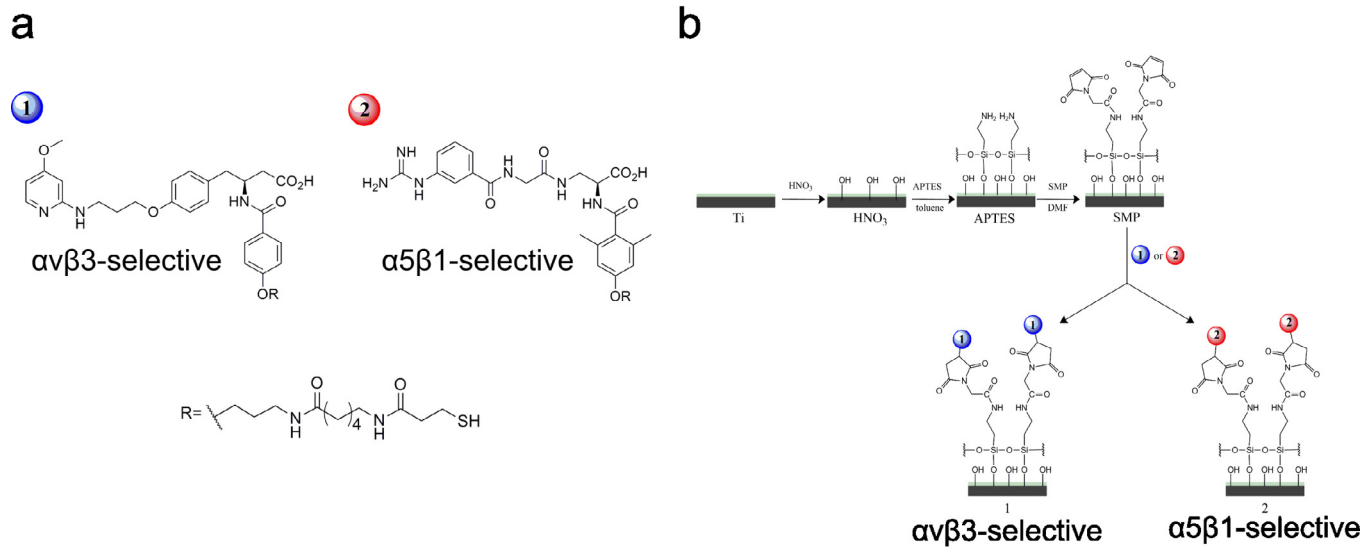

Fig. 1. (a) Chemical structure of the αvβ3-selective (1) and α5β1-selective (2) peptidomimetic ligands. (b) Schematic representation of the surface functionalization strategy.

mechanical and biochemical interactions with cells than the native surface of the implant. These approaches comprise both inorganic, such as calcium phosphate coatings [6,7], and organic modifications. Organic coatings are often based on grafting biomolecules derived from the extracellular matrix (ECM) [8,9], thus mimicking the natural environment that supports and mediates cell functions on the metallic surface. Such biomimetic strategy relies on the fact that cells are capable of interacting with their surroundings through membrane receptors, such as integrins. This family of heterodimeric transmembrane proteins provides a communication pathway from the environment to the nucleus of the cell (outside-in signaling), and *vice versa* (inside-out signaling), which controls proliferation, migration, differentiation and apoptosis of cells [10,11]. Hence, by functionalizing the surface of the material with receptor-binding cues it is possible to dictate cell fate and direct a favorable osteointegration of the implant.

Several approaches have been explored to mimic natural ECM, from complex full-length proteins [12] to minimal linear cell adhesion motifs [13,14]. Between these strategies, many alternatives have been developed with the aim of improving biofunctionality, affinity and selectivity of the ligand, while reducing the complexity and immunogenicity typical of natural ECM proteins. Multiple peptide motifs [15,16], peptide mixtures [17], branched [18,19] or cyclic peptides [20–23], and engineered protein fragments [24,25] have been designed to overcome these limitations but debate is still open on which is the best strategy [26]. Covalent immobilization of peptides has been proven reliable in terms of *in vitro* performance, promoting adhesion, proliferation and differentiation of OB-like cells [16,19,27,28]. Moreover, some *in vivo* studies already demonstrated the efficacy of this functionalization strategy in terms of retention of peptide bioactivity and consequent increase in bone-implant contact area compared to uncoated Ti [29]. Nevertheless, it is also demonstrated that the use of small sequences of peptides bears several limitations such as low specificity and affinity for cellular receptors, and low stability to enzymatic degradation [30]. To solve these issues, a promising alternative is the use of synthetic peptidomimetics [31,32]. These artificial ligands show almost no immune reaction in the body, high stability in serum and can be designed to have high affinity for a specific integrin subtype.

In this regard, the development of αvβ3- or α5β1-selective peptidomimetics for surface coating was recently reported by us [33,34]. These compounds, which showed highly specific affinity for one integrin subtype (Fig. 1a), were able to promote selective cell adhesion of αvβ3- or α5β1-expressing fibroblasts on gold [33] and titanium [34] substrates. Both αvβ3 and α5β1 heterodimers have crucial functions in bone biology: first, the β1 subfamily is the most highly expressed integrin subfamily by osteoprogenitor and OB cells [35], and the αvβ3 the most abundant integrin expressed by adherent sarcoma osteogenic (SaOS-2) cells on Ti [36]; secondly, their activation is involved in many processes required for bone development onto a solid substrate, such as focal contacts formation [37–39], force sensing and mechanotransduction [38–41], and osteogenesis [42,43].

Based on these premises, we propose the immobilization of integrin-binding peptidomimetics on Ti as a feasible and powerful strategy to mimic bone ECM, and thus improve OB adhesion and accelerate osteointegration of implants. The aim of this work was to investigate this strategy by covalently anchoring compounds **1** and **2** (Fig. 1a) onto Ti surfaces, and characterizing the behavior of SaOS-2 cells on these bioactive surfaces. Covalent immobilization of the biomolecules was achieved through a simple silanization protocol with 3-(aminopropyl)-triethoxysilane (APTES) (Fig. 1b). The physicochemical properties of the surfaces and the presence of the ligands were characterized by contact angle and surface energy calculations, roughness measurements, X-ray photoelectron spectroscopy (XPS) and fluorescent labeling methods. Cell response was evaluated *in vitro* both at short and long incubation times, in terms of adhesion (number of cells attached, cell spreading and cytoskeletal organization), proliferation, and differentiation (alkaline phosphatase production and mineralization). The biological performance of the peptidomimetics was compared to surfaces coated with vitronectin (VN) or fibronectin (FN), since these proteins, abundant in bone ECM, have been proved to be also αvβ3- [44] or α5β1- [45] binding proteins, respectively.

2. Materials and methods

2.1. Preparation of functionalized Ti surfaces

Cylindrical CP Ti bars (diameter: 10 mm) were obtained from Technalloy S.A. (Sant Cugat del Vallès, Spain). Ti disks (thickness: 2 mm) were prepared by turning, smoothed with silicon carbide grinding papers (Neuertek S.A., Eibar and Beortek S.A., Asua-Erandio, Spain) and polished with suspension of alumina particles (1 μm and 0.05 μm particle size) on cotton clothes. Smooth mirror-like surfaces were obtained, and ultrasonically rinsed with

cyclohexane, isopropanol, distilled water, ethanol and acetone and stored dried. Prior to silanization, samples were passivated with 65% (v/v) HNO_3 for 1 h and ultrasonically cleaned with distilled water, ethanol and acetone. Straight after the oxidizing treatment, silanization was performed by immersing samples in 2% (v/v) APTES (Sigma–Aldrich, St. Louis, MO, USA) in anhydrous toluene (Sigma–Aldrich) at 70 °C for 1 h under nitrogen atmosphere, followed by 5 min ultrasonic rinsing with toluene. Next, samples were rinsed with toluene, distilled water, ethanol and acetone. The silane layer was finally cured at 120 °C for 5 min. Coupling of the crosslinking agent *N*-succinimidyl-3-maleimidopropionate (SMP) (Alfa Aesar, Karlsruhe, Germany) in *N*,*N*-dimethylformamide (DMF) was done by soaking disks in 7.5 M solution for 1 h at room temperature (RT) and rinsing with DMF, distilled water, ethanol and acetone afterwards. Both silanization and SMP coupling were performed under agitation and were followed by rinsing with distilled water, ethanol and acetone. Peptidomimetics **1** and **2** were synthesized as previously described [33,46]. Their immobilization on Ti surface was performed by first dissolving the biomolecules in phosphate buffered saline (PBS) at 100 μM [33] and pH 6.5, and then depositing 100 μL of these solutions overnight on samples at RT. VN and FN (both from Sigma–Aldrich) were used as positive controls and were coated to Ti at 50 μg/mL in PBS at pH 9.5. The coating treatment was followed by rinsing three times with PBS. Uncoated polished Ti disks were selected as negative controls. Surfaces were named according to the coating molecule. The process of surface functionalization is summarized in Fig. 1b.

2.2. Characterization of surface physicochemical properties

White light interferometry in vertical scanning interferometry mode (Wyko NT9300 Optical Profiler, Veeco Instruments, New York, NY, USA) was used to evaluate roughness of Ti disks after polishing treatment. The average roughness (R_a) of each sample was measured in three randomly chosen points of the disk. Data were analyzed with Wyko Vision 4.10 software (Veeco Instruments). Moreover, the sessile drop method was used to measure static contact angle of ultrapure Milli-Q water and diiodomethane (volume of wetting liquids: 1 μL) (Contact Angle System OCA15 plus, Dataphysics, Filderstadt, Germany), allowing the calculation of surface energy with Young-Laplace and Owen-Wendt equations [47,48]. Contact angle values of 3 drops per sample were obtained using Laplace–Young fitting with SCA 20 software (Dataphysics).

2.3. Chemical composition of the surfaces by XPS

XPS was used to analyze chemical composition of Ti surfaces. The system (SPECS Surface Nano Analysis GmbH, Berlin, Germany) was equipped with a non-monochromatic Mg anode X50 source, operating at 150 W and a Phoibos 150 MCD-9 detector. Detector pass energy was fixed at 25 eV with 0.1 eV steps to record high resolution spectra at a pressure below 7.5×10^{-9} mbar. Casa XPS software (Version 2.3.16, Casa Software Ltd., Teignmouth, UK) was used to do fitting and peak integration of spectra. All binding energies were analyzed calibrating to the C1s signal located at 284.8 eV.

2.4. Fluorescent labeling of surface-bound peptidomimetic molecules

In order to detect the presence of the bioactive molecules on the functionalized Ti surfaces, a labeling protocol with a fluorescent tag was carried out [15]. Each peptidomimetic has a carboxyl group in its chemical structure (Fig. 1a) that is available for coupling with a fluorescently-labeled amine. To this end, functionalized surfaces were incubated with 1-ethyl-3-(3-dimethylaminopropyl)carbodiimide (EDC)·HCl (5 mM) (Sigma–Aldrich) and *N*-hydroxysulfosuccinimide (sulfo-NHS) (7.5 mM) (Thermo Scientific, Waltham, MA, USA) in PBS at pH 6.5 for 15 min under gentle shaking. After 3 times washing with PBS at pH 7.4, samples were immersed in a 0.1 mM solution of Oregon Green® 488 Cadaverine (Life Technologies, Paisley, UK) in PBS for 2 h under agitation. Finally, Ti disks were rinsed 5 times with Milli-Q water and examined under a fluorescence microscope (Nikon E600, Tokyo, Japan). Three images per disk were taken and fluorescence intensity quantified with Fiji/Image-J package (NIH, Bethesda, MD, USA) [49].

2.5. Cell culture

SaOS-2 cells were cultured in Mc Coy's 5A medium supplemented with 10% (v/v) fetal bovine serum (FBS), 50 U/mL penicillin, 50 μg/mL streptomycin and 1% (w/v) L-glutamine. Cells were maintained at 37 °C, in a humidified atmosphere containing 5% (v/v) CO_2 and culture medium was changed twice a week. Upon reaching confluence, cells were detached by trypsin-EDTA and subcultured into a new flask. Cells at passages between 25 and 35 were used to carry out all the experiments. All reagents were purchased from Sigma–Aldrich, unless otherwise noted.

2.6. Cell adhesion

Adhesion of cells on Ti surfaces was evaluated after 4 h of incubation in serum-free medium by quantification of attached cells *via* enzymatic assay. Prior to seeding, samples were rinsed three times with PBS and blocked in 1% (w/v) bovine serum albumin (BSA) for 30 min at RT to avoid non-specific protein adsorption. Samples tested for mechanical stability of the coating had been ultrasonicated for 1 h in Milli-Q water prior to PBS washings and BSA blocking. Ti disks were moved to 48-well plates wells, cells were seeded at 5×10^4 cells/mL and incubated at 37 °C and 5% (v/v) CO_2 containing atmosphere. 4 h post-seeding non-adherent cells were washed off by gently rinsing with PBS, and remaining cells were lysed with 300 μL/disk mammalian protein extraction reagent (M-PER). Enzymatic activity of lactate dehydrogenase (LDH) was quantified by colorimetric assay (Cytotoxicity Detection Kit (LDH), Roche Diagnostics, Mannheim, Germany), using a multimode microplate reader (Infinite M200 PRO, Tecan Group Ltd., Männedorf, Switzerland). Cell number was obtained using a standard curve.

2.7. Cell proliferation

After functionalization, samples were rinsed with PBS and blocked with 1% (w/v) BSA, following the same protocol described for cell adhesion assays. SaOS-2 cells were then plated at a concentration of 2×10^4 cells/mL in serum-free medium and incubated for 4 h. Medium was aspired 4 h post-seeding and FBS-supplemented medium was added. On days 3, 7 and 14, medium was replaced with Alamar Blue-containing medium (10% (v/v), Invitrogen life technologies, Merelbeke, Belgium) for 3 h and fluorescence of the dye quantified afterward according to manufacturer instructions. This minimally-toxic redox indicator changes color and fluorescence in response to chemical reduction of the medium, which results from continued growth of cells.

2.8. Immunofluorescence analysis of cell morphology

Coated Ti surfaces were rinsed with PBS and blocked with BSA, and SaOS-2 cells plated on samples as previously explained. Cells were allowed to attach for 4 h in serum-free medium, and subsequently fixed with paraformaldehyde (PFA, 4% w/v in PBS) for 20 min, permeabilized with 500 μL/disk of 0.05% (w/v) Triton X-100

in PBS for 20 min and blocked with 1% BSA (w/v) in PBS for 30 min. Actin fibers and nuclei were stained by incubating with rhodamine-conjugated phalloidin (1:300, in Triton 0.05% (w/v) in PBS) for 1 h and with 4′,6-diamidino-2-phenylindole (DAPI) (1:1000, in PBS-Glycine 20 mM) for 2 min at RT in the dark, respectively. Between all steps, samples were rinsed three times with PBS-Glycine for 5 min. Ti disks were mounted and examined under a fluorescence inverted microscope (AF7000, Leica, Germany) and images processed using Fiji/Image-J package.

2.9. Evaluation of osteogenic differentiation

Differentiation of OB-like cells was assayed by measuring early markers of both differentiation and mineralization. To this end, SaOS-2 cells were plated in the same conditions as in the proliferation assays. The early marker ALP was quantified using *p*-nitrophenyl phosphate as a substrate and measuring the amount of *p*-nitrophenol produced (SensoLyte® pNPP Alkaline Phosphatase Assay Kit, AnaSpec Inc., Fremont, CA, USA) on day 7 and 14. Briefly, at these time points, samples were rinsed with PBS to remove non-adherent cells and M-PER (300 μL/well) was added. Cell lysates were diluted and enzyme activity measured according to manufacturer instructions. ALP activity was normalized to cell number. Calcified matrix was detected on day 21 using Alizarin Red S (ARS) staining method (Sigma–Aldrich). In this case, 4 h after seeding 2×10^4 cells/mL in serum-free medium, culture medium was replaced with osteogenic medium (OG-medium), supplemented with 10 mM β-glycerophosphate, 50 μg/mL ascorbic acid, and 100 nM dexamethasone (Sigma–Aldrich). At the end of the incubation time, samples were washed with PBS and adhered cells fixed with 4% (v/v) PFA at RT for 20 min. Ti disks were then washed twice with Milli-Q water and 500 μL/well of 40 mM ARS (pH 4.2) was added. Plates were incubated with the dye at RT for 20 min while gently shaking. Prior to quantification, excess dye was washed off using copious washings with Milli-Q water. Cetylpyridinium chloride (CPC) buffer (10% (w/v) in 10 mM NaH_2PO_4, pH 7) was added (300 μL/well) at RT for 30 min to elute stain. Supernatant was then collected, diluted 1:2 with CPC buffer and 100 μL aliquots were plated to measure absorbance at 570 nm.

2.10. Statistical analysis

All experiments were performed in triplicates and repeated at least in two independent experiments. Statistical comparison of values was based on ANOVA using Tukey's test for pair-wise comparison with $p < 0.05$. Differences were also analyzed by non-parametric Mann–Whitney test. Values of all graphs are reported as mean ± standard deviation. The software used for statistical analysis was Minitab 16.2.2 Statistical Software (www.minitab.com, Minitab Inc.).

3. Results and discussion

3.1. Functionalization strategy and surface characterization

To ensure the successful covalent attachment of the biomolecules on Ti surfaces, a straightforward protocol based on silanization was carried out (Fig. 1b). Ti samples were passivated with a standard HNO_3 treatment, which yields a homogenous Ti oxide (TiO_2) layer on the surface. Such layer spontaneously forms hydroxyl groups that are necessary for the subsequent silanization step [50]. Oxidation with HNO_3 was chosen because it is done under mild conditions and it does not modify the surface roughness, as observed with more aggressive methods, such as acidic or alkaline etchings [51–53]. Silanization with APTES was performed according to well-established protocols, with some minor modifications [54,55]. Conversion of the terminal amino groups into maleimide functionalities with SMP finally allows the chemoselective binding of the mimetics *via* the anchoring thiol groups (Fig. 1a). Immobilization of the peptidomimetics is done overnight at pH 6.5 in order to optimize the coupling yields of the Michael-addition [55] and to avoid disulfide bridge formation. It should be highlighted that the presence of an aminohexanoic acid spacer unit in the peptidomimetics structure ensures an adequate accessibility and presentation of the active motifs for interaction with cell receptors [20,23].

Roughness of the implant surface deeply affects cell behavior [3], influencing adhesion, proliferation and differentiation of cells. Rough surfaces (R_a at micro-level) have been proved to stimulate a positive response of OB-like cells on Ti and Ti alloys [56]. However, as the aim of this study was to evaluate cell response to bioactive ligands, samples were polished until achieving homogeneous smooth surfaces with R_a values below 20 nm. Moreover, such mirror-like surfaces were chosen as reference topography because the biological effect displayed by surface-bound bioactive molecules has been proved to be more evident on smoother substrates than on rougher ones [23]. White light interferometry in vertical scanning mode was used to measure R_a values of samples

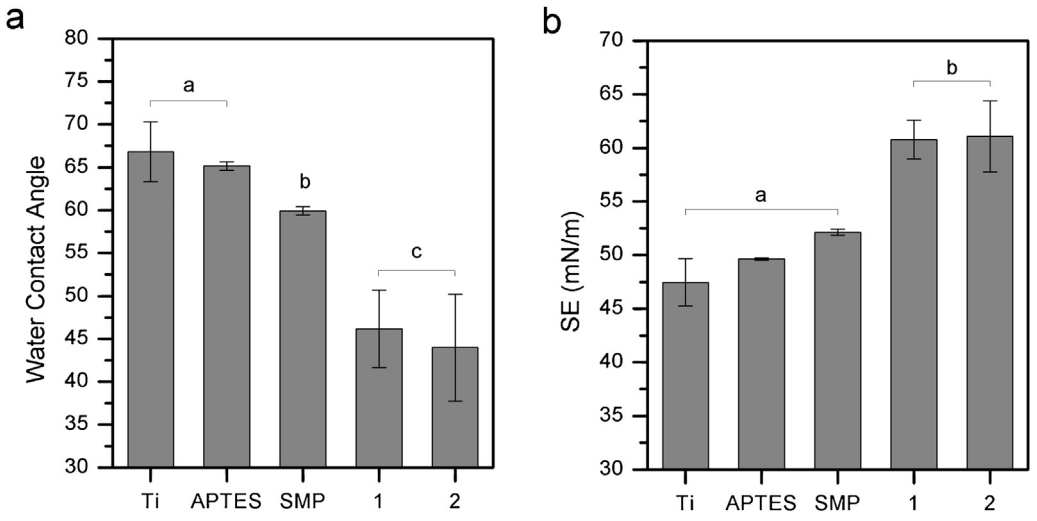

Fig. 2. Contact angle values of water on Ti disks (a) and calculated surface energy (SE) (b) in each step of the functionalization process (APTES, SMP, 1 and 2 correspond to surfaces in Fig. 1b). Columns marked with different letters belong to statistically different groups (p-value < 0.05).

Table 1
Atomic percentage composition and N/Si atomic ratio of Ti surfaces throughout each step of the functionalization process.

	Elemental composition (atomic %)					N/Si
	O 1s	Ti 2p	C 1s	Si 2p	N 1s	
Ti–HNO_3 treated	63.46 ± 1.65	15.89 ± 0.78	20.11 ± 2.54	0.06 ± 0.07	0.49 ± 0.12	
APTES	40.05 ± 5.13	7.15 ± 1.44	39.39 ± 7.78	7.34 ± 1.20	6.07 ± 0.56	0.83
Compound 1	43.03 ± 8.95	5.26 ± 1.20	40.76 ± 9.68	4.50 ± 0.58	6.46 ± 0.69	1.44
Compound 2	46.03 ± 4.09	6.05 ± 0.78	36.87 ± 3.69	4.54 ± 0.72	6.51 ± 0.68	1.43

before and after the polishing process, as well as after HNO_3 activation (Table S1 in the Supporting Information). Data indicate that roughness of samples, once reduced by the polishing process, is not affected by the passivation treatment. Also the following functionalization steps do not affect topography of samples (data not shown), in agreement with previous studies [57]. These observations allowed us to exclude the influence of surface topographical features of the on cell behavior.

Hydrophilicity of the substrate is another fundamental parameter affecting cell response [58]. Static contact angle of water and diiodomethane were measured, and surface energy (SE) was calculated in each step of the functionalization protocol (Fig. 2). Silanization did not change the wettability of the samples, and coupling of the crosslinker resulted only in a slight decrease of water contact angle. However, upon binding compound **1** or **2** to the surface, a statistically significant increase in hydrophilicity was observed, probably due to the presence of hydrophilic polar groups of the peptidomimetics. On the other hand, contact angle of diiodomethane does not change significantly through the entire functionalization process (data not shown). Contact angle results, although not suitable to distinguish between peptidomimetics, confirmed the binding of compounds **1** and **2** through a clear decrease in water contact angle. Furthermore, calculated values of SE of peptidomimetics-functionalized surfaces are almost coincident, indicating that differences in cell response between compounds **1** and **2** cannot be related to differences in these physicochemical properties.

Chemical composition of the outer layer of the surface throughout the functionalization steps was monitored using XPS analysis (Table 1). Control HNO_3-treated Ti disks showed the characteristic peaks of Ti 2p (not shown) and O 1s (Fig. 3b) of TiO_2 layer [50]. The C 1s signal is due to the presence of organic contaminants from the environment. Upon addition of the aminosilane, N 1s and Si 2p peaks appear, at 401.0 eV (Fig. 3c) and 103.8 eV (not shown) respectively, while both oxygen and titanium peaks' intensities decrease (Table 1). Both the appearance of N and Si, and the reduction of Ti and O peaks have been associated to the formation of the siloxane layer on the metal [54]. The N/Si ratio is slightly lower than expected, as already observed in the literature [19,55]. Xiao et al. [55] explained this discrepancy with the partial loss of amine groups after polymerization of silanes. C 1s spectrum deconvolution of Ti samples showed the presence of three peaks (Fig. 3a): a main peak attributed to aliphatic carbons (—CH_2—CH_2—) from atmospheric contaminants at 284.4 eV; a smaller peak at 286.0 eV, associated to carbons bound to amines (—CH_2—NH_2), alcohols (—CH_2—OH) or alkoxy or ether groups; and a third peak at 288.2 eV, due to carbonyl groups (—C═O). Silanization with APTES increased the contribution of the peak at 286 eV from 18% to 28% (Table S2 in the Supporting Information), owing to the presence of amine-bound carbons on the aminosiloxane layer. Also the appearance of a new O 1s peak at 533.5 eV, resulting from siloxane groups, is consistent with a successful silanization (Fig. 3b) [54]. The deconvolution of N 1s spectrum identifies two peaks characteristic of primary amines (Fig. 3c): protonated amino groups at 402.7 eV, as observed in previous studies [19], and unprotonated amino groups at 400.7 eV, also in agreement with literature data [16]. All together, these data proved the efficiency of the silanization protocol. The binding of both peptidomimetics to Ti was accompanied by a decrease in the Ti 2p and Si 2p atomic percentages (Table 1), indicating the presence of the biomolecules. Deconvolution of the C 1s spectrum further confirmed the presence of compounds **1** and **2**: the highest energy peak at 288 eV increased its contribution, from 7.5% in the APTES surface to 18% and 20%, in compound **1**- and **2**-coated surfaces, respectively (Fig. 3a, Table S2 in the Supporting Information). This increase is consistent with new amide functionalities (—NH—C═O), and imide groups (O═C—N—C═O) corresponding to the crosslinker [55,59]. The attachment of the ligands was also evidenced by an increase in the high energy peak of O 1s at 533 eV, which is associated to carbonyl groups (Fig. 3b, Table S2 in the Supporting Information). However, this peak cannot be deconvoluted separately from the siloxane signals. Amide groups were observed in the N 1 s spectra at energies close to 401 eV but this signal may overlap with free unprotonated amino groups from the silane. The positively charged aminopyridine and guanidine groups of compounds **1** and **2**, respectively, were located at 402.0 eV (Fig. 3c, Table S2 in the Supporting Information) [54].

In addition to XPS analysis, fluorescent labeling of the peptidomimetic compounds was done to corroborate their anchoring to the surfaces. Briefly, after coupling a fluorescent amine to the available carboxyl group of compound **1** and **2**, images of the Ti disks were taken and fluorescence intensity quantified. Apart from isolated spots, probably related to unbound fluorescent marker leftovers, uncoated Ti disks showed no fluorescence at all. On the contrary, the intensity in fluorescence was significantly increased on surfaces coated with either compound **1** or **2** (Fig. S1 in the Supporting Information).

3.2. *Peptidomimetics coating fosters adhesion and spreading of SaOS-2 cells on Ti*

The effect of the integrin-binding peptidomimetics on short-time cell adhesive events was evaluated by quantifying the number and projected area of OB-like cells adhering on Ti after 4 h of incubation. In order to compare the biological performance of peptidomimetics with the effect displayed by coating the surfaces with natural ECM proteins, the biological assays included two positive controls, consisting of VN- and FN-coated Ti surfaces. VN and FN are involved in a complex and rich series of events in bone biology [44,45,60–62], and their cell-adhesive capacity has been proved to be primarily mediated by αvβ3 and α5β1 integrin receptors, respectively [35,63,64]. Thus, VN and FN coated surfaces constitute good substrate models of bone ECM. As shown in Figs. 4a and 5, the anchoring of peptidomimetics to Ti statistically ($p < 0.05$) increased both the number and the area of adherent SaOS-2 cells, compared to uncoated Ti. Mechanical stability of the peptidomimetics coating was also tested by ultrasonication for 1 h in Milli-Q water prior to cell seeding. Interestingly, no significant differences in cell adhesion were observed after this treatment (surfaces 1s and 2s, Fig. 4a), thus proving the stability of the functionalization system toward mechanical and thermal stresses in an aqueous environment. Furthermore, it is noteworthy that both peptidomimetics, improved cell adhesion on Ti surfaces to the same level shown by

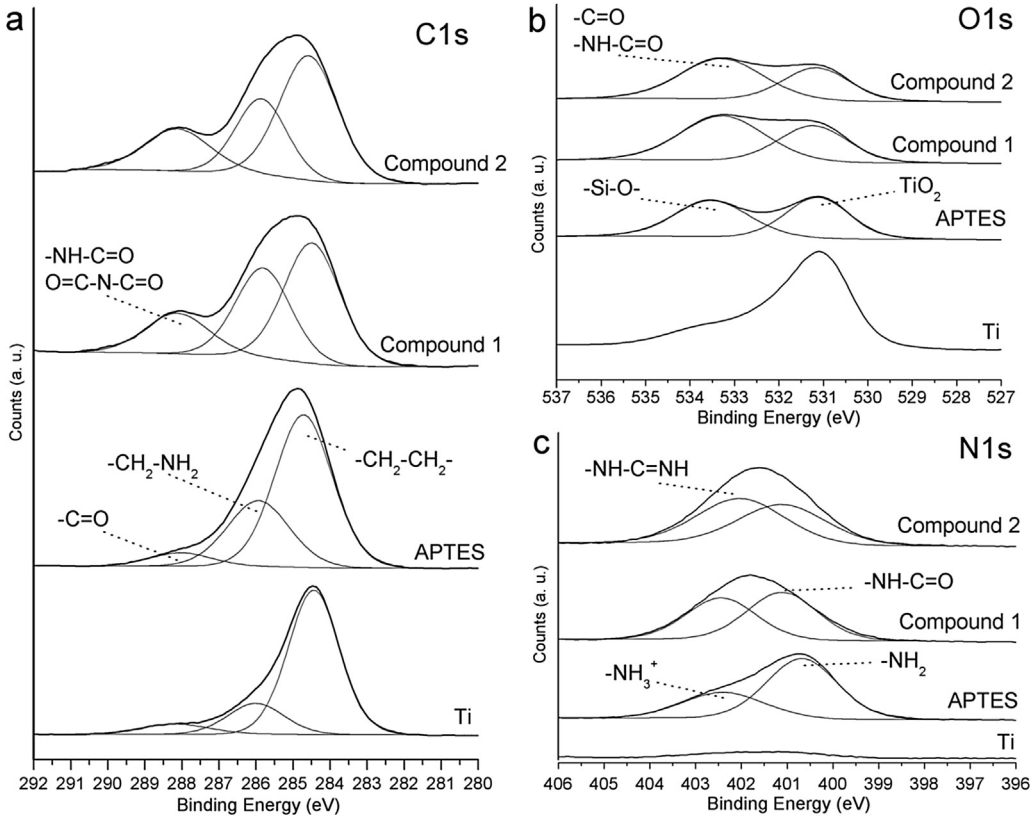

Fig. 3. Deconvolution of XPS spectra of C 1s (a), O 1s (b) and N 1s (c) for the Ti surface throughout the steps of the functionalization process.

ECM-protein coatings (Fig. 4a). Such improvement is solely due to the presence of the biomolecules, as no enhancement of cell adhesion efficiency was observed in any previous step of the functionalization process, as demonstrated by us in a recent study (Fig. S4 in [16]). The analysis of the projected area of cells also revealed a clear effect of the peptidomimetics coating (Fig. 5). Mean cell area on the surfaces coated with the peptidomimetics was significantly higher ($p < 0.05$) than the one reached on uncoated Ti. As evidenced from the immunofluorescence study of actin cytoskeleton, almost all SaOS-2 cells attached to control Ti showed a completely rounded shape. On the contrary, high cell spreading and a fully developed cytoskeleton were visible on both peptidomimetic-functionalized surfaces (Fig. 5). Although adhesion and focal contact formation of OBs on several substrates has been described to be mainly α5β1-mediated [25,65,66], we found that both αvβ3- and α5β1-selective surfaces promoted the same extent of attachment and spreading of SaOS-2 cells. In fact, a previous study analyzing integrin expression of SaOS-2 cells on Ti reported high expression of α5 and β1 subunits, and of αvβ3, which was the integrin with the highest level of expression [36]. Therefore, it should not come

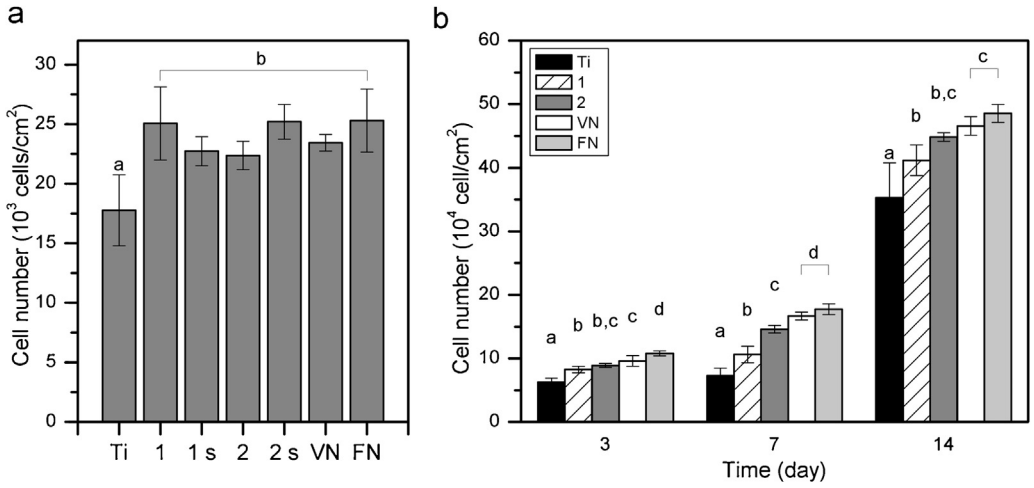

Fig. 4. (a) Number of SaOS-2 cells adhered on Ti surfaces after 4 h of incubation in serum-free medium. Cells were quantified *via* LDH enzymatic assay. The letter "s" denotes the samples were subjected to ultrasonication in water for 1 h prior to cell seeding. (b) Proliferation of SaOS-2 cells on Ti surfaces after 3, 7 and 14 days of culture. Quantification of cell numbers was done with Alamar Blue assay. APTES, SMP, 1 and 2 correspond to surfaces in Fig. 1b. Columns marked with different letters belong to statistically different groups (p-value < 0.05).

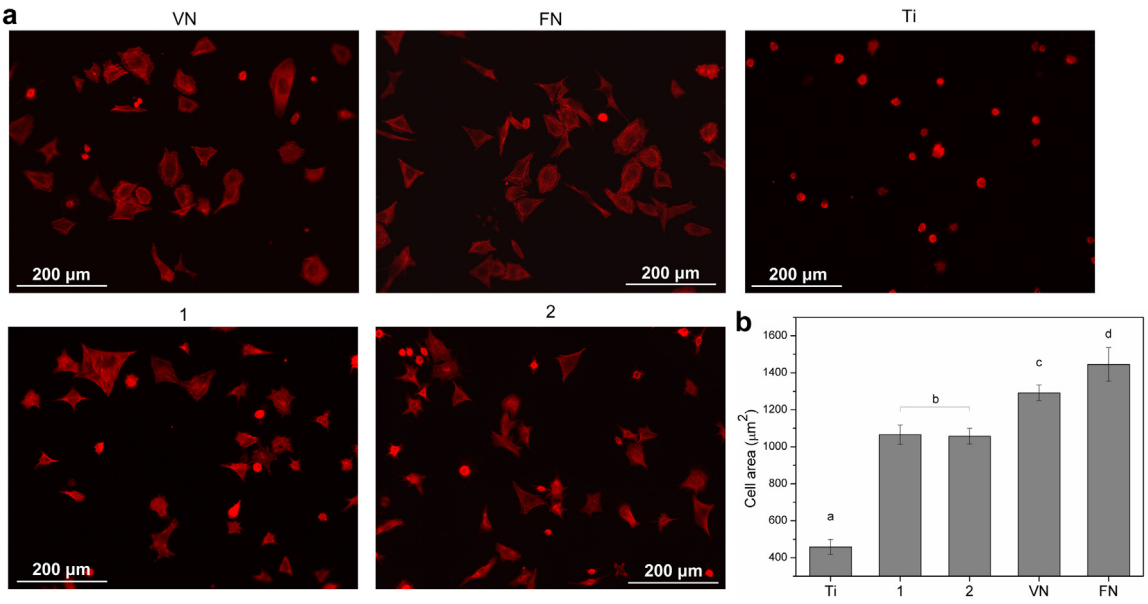

Fig. 5. Spreading of SaOS-2 cells adhered on Ti surfaces after 4 h of incubation in serum-free medium. (a) Immunofluorescent staining of F-actin of SaOS-2 cells. Scale bar: 200 μm. (b) Quantification of cell area is obtained by calculating the mean projected cell area in a (5 mm × 5 mm) central section of each disk. APTES, SMP, 1 and 2 correspond to surfaces in Fig. 1b. Columns marked with different letters belong to statistically different groups (p-value < 0.05).

as a surprise that both peptidomimetics have the potential to support the adhesion and spreading of OB-like cells, through the activation of these two surface receptors, which are known to play a key role in different phases of focal adhesions maturation [37]. Although these integrin subtypes play distinct roles in cell adhesive processes [37–39,41,67], both α5β1 and αvβ3 have been described to support attachment, spreading and focal contacts formation on a solid substrate [37]. However, determining the exact role of each integrin subtype requires a deeper study of the signals activated by receptors, and it is beyond the aim of this study.

3.3. Proliferation of SaOS-2 cells is supported on the coated Ti surfaces

Proliferation of SaOS-2 cells on functionalized substrates was quantified at three time points by Alamar Blue viability assay (Fig. 4b). Proliferation rate was increased by both peptidomimetics, compared to the uncoated Ti. This behavior was statistically significant ($p < 0.05$) at all time points for both compound **1** and compound **2**. Coating of Ti with the ECM proteins yielded the highest proliferation rates. The general trend of cell growth, which is maintained throughout the 14 days of incubation, was uncoated Ti < compound **1** < compound **2** < VN < FN. Taking into account that both FN- and compound **2**-coated surfaces may preferentially interact with SaOS-2 cells through the α5β1 integrin, our data suggests that this receptor may have an important role in promoting proliferation of OB-like cells on Ti. In this regard, a previous report highlighted the role of α5β1 in regulating the expression of activator protein-1 (AP-1) transcription factors, c-*fos* and c-*jun*, which are crucial in OB proliferation [68]. In this study, it was shown that by blocking α5β1 integrin before plating cells on FN, c-*fos* mRNA expression was decreased to control levels [69]. The same integrin receptor was also shown to play an important, though not critical, role in mesenchymal stem cells proliferation [70]. However, in this case blocking of α5β1 did not prevent stem cells from growing on FN, as additional signals provided by the full-length protein were sufficient to support cell proliferation. Thus, the authors concluded that highly selective ligands are required to study specific biological effects of the receptor. Our data demonstrate that proliferation levels attained on the surfaces functionalized with the α5β1-selective ligand **2** are not far from the rates reached using a full-length protein, thereby indicating that binding α5β1 might be sufficient to induce cell growth on the material. The role of the αvβ3 receptor in this process is not clear: Martino et al. [70] reported increased proliferation of stem cells after blocking this integrin, while other works showed enhanced proliferation rates of OB-like cells on surfaces coated with αvβ3-binding cyclic RGD peptides [71,72]. In this work, αvβ3-selective surfaces efficiently supported SaOS-2 proliferation at all time points, though to a lower extent than α5β1-selective surfaces.

3.4. POsteogenic differentiation and mineralization are stimulated by integrin-binding peptidomimetics

ALP activity and the production of calcium were studied as early markers of osteogenic differentiation and mineralization of OB-like cells, respectively. SaOS-2 cells have been shown to express ALP when cultured on Ti and its alloys [36,73–75], presenting a peak of expression between the first and the third week of culture, depending on the substratum. Thus, the expression of this marker was quantified after incubating SaOS-2 cells for 7 and 14 days on Ti surfaces, and normalized to cell number (Fig. 6a). On day 7, a trend toward higher ALP production was observed for both peptidomimetics in comparison to uncoated Ti, although this increase was not statistically significant. Both ligands supported the same levels of ALP production as full-length VN. At this time point, the lowest expression of the enzyme was found on FN-coated Ti ($p < 0.05$). Taking into account the trends in cell growth previously observed (Fig. 4b), on day 7 FN seems to encourage cell proliferation, rather than expression of this osteoblastic marker.

The positive tendency observed in ALP production by the peptidomimetics was maintained after 14 days of incubation, reaching a statistically higher expression of ALP for surfaces coated with compound **2** compared to uncoated Ti. Moreover, no differences in ALP activity were detected between the use of the peptidomimetics or native ECM proteins. Overall, the peptidomimetics were able to support the same (peptidomimetic **1**) or higher (peptidomimetic **2**, $p < 0.05$) level of ALP expression compared to uncoated Ti.

Alizarin Red S staining method allows for the detection of the calcium content of the ECM, which is directly correlated to the

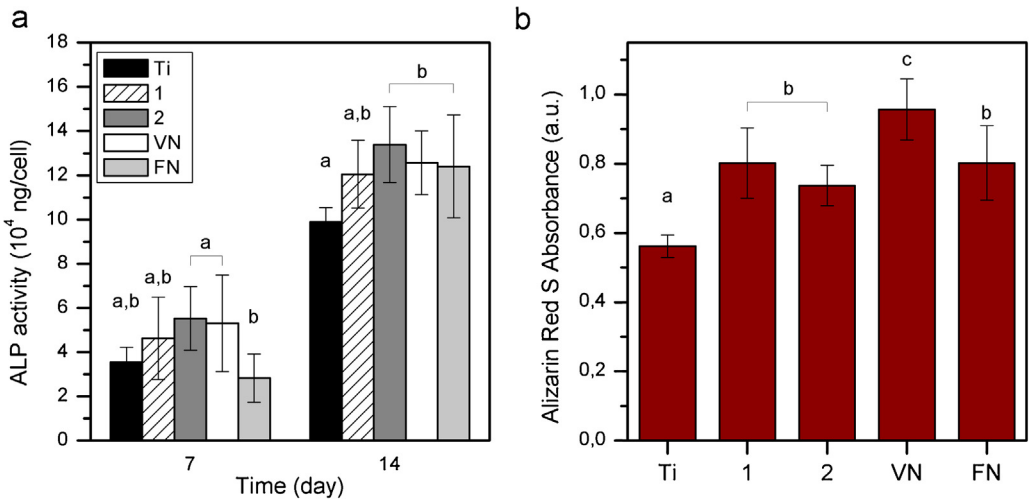

Fig. 6. (a) Alkaline phosphatase activity (ALP) quantified after 7 and 14 days of incubation by pNPP conversion. (b) Quantification of calcium production of SaOS-2 cells, cultured for 21 days on Ti surfaces. Columns marked with different letters belong to statistically different groups (p-value < 0.05).

degree of mineralization of the matrix. This late marker of differentiation has been already used when culturing cells on Ti to demonstrate the enhancement of matrix calcification by several modification treatments [76]. In our study, functionalized and protein-coated samples showed a diffuse mineralization pattern, which is characteristic for osteosarcoma cell lines [77], while control Ti surfaces only supported a very poor mineralization (Fig. 6b and Fig. S2 in the Supporting Information). In order to quantify the production of calcium, the dye was eluted and its absorbance measured (Fig. 6b), corroborating the results of the microscope observation (Fig. S2 in the Supporting Information). Both peptidomimetics induced mineralization of SaOS-2 cells' ECM, significantly higher ($p < 0.05$) than the uncoated Ti surface. The fact that both VN- and compound **1**-functionalized Ti surfaces support calcification of the matrix is particularly relevant, as it suggests an important role of integrin αvβ3 in the osteogenic differentiation of pre-osteoblasts. These results are not in agreement with previous studies, which describe that integrin α5β1 induces differentiation of OBs (*e.g.* mineralization), while αvβ3 suppresses it [25,66,78]. Nonetheless, the αvβ3 receptor, which is usually associated to the bone resorptive activity of osteoclasts, has also been proved to have a fundamental role in matrix mineralization: previous works showed that its perturbation led to a decrease in osteoblast matrix mineralization of 65%, while perturbation of integrin α5 or β1 only caused a decrease of 20% and 45%, respectively [79]. The fact that the pattern of integrin expression strongly depends on cell type, incubation time, and the nature and physicochemical properties of the substrate, may justify these discrepancies. The use of undifferentiated cell types (*i.e.* mesenchymal stem cells), integrin-blocking antibodies and a broader biological study would give deeper information on the specific roles of these integrins in bone biology; these approaches are currently on-going in our laboratory. Finally, it should be pointed out that no clear inverse relationship between proliferation and differentiation was observed. This was expected as SaOS-2 cells undergo a deregulation of cell growth and gene expression, which may lead to high proliferation rates and differentiation into the osteoblastic lineage at the same time [80].

On the whole, our studies have shown that coating Ti surfaces with αvβ3- or α5β1-binding peptidomimetics increases the attachment, spreading, cytoskeletal formation, proliferation, ALP activity, and matrix mineralization of SaOS-2 cells on the surfaces. From our studies, it can be concluded that both peptidomimetic ligands equally stimulate OB-like cell adhesion, growth and differentiation on metallic substrates. Furthermore, it is of great relevance that the biological performance of peptidomimetic molecules is comparable to the response elicited by complex full-length proteins of bone ECM. To the best of our knowledge, this is the first report describing such unprecedented activity for synthetic low-molecular-weight organic molecules on Ti substrates. Our study suggests that a successful mimicry of ECM functions can be attained by addressing cell receptors, such as integrins, with small and selective ligands, instead of complex full-length proteins. These results, together with the high stability to enzymatic degradation displayed by peptidomimetics, confirm the potential of this strategy to increase the osteointegration of metal implants *in vivo*.

4. Conclusions

In this work, we have reported a straight-forward strategy of functionalization to provide implant materials with osteoinductive properties. In particular, CP Ti disks were grafted with two highly active integrin-binding peptidomimetics. The successful immobilization of the biomolecules was proven by XPS and fluorescent studies, and the coatings were shown to be mechanically stable. Noteworthy, these ligands significantly improved the adhesion, proliferation and differentiation of OB-like cells on Ti surfaces almost to the same extent as observed for native ECM proteins. There were no significant differences between the two peptidomimetics. On the whole, the positive biological outcome observed on the biofunctionalized-samples indicates that single receptor-binding cues would be able to support the process of osteointegration of metals and opens promising prospects for diverse clinical applications in dentistry and orthopedics. Furthermore, the outstanding biological responses attained by such small and specific synthetic molecules, similar to those supported by complex and unspecific full-length proteins, is of great relevance: this simplified integrin-selective model allows to direct integrin-selective biological responses, paving the way for a much more specific response-oriented design of biomaterials.

Acknowledgements

The authors acknowledge the Spanish Government for financial support (Project: MAT2012-30706), co-funded by the European Union through European Regional Development Funds, and the Government of Catalonia (SGR2009 1039). R.F. thanks the Government of Catalonia for financial support through a predoctoral fellowship. C.M.-M. thanks the support of the Secretary for

Universities and Research of the Ministry of Economy and Knowledge of the Government of Catalonia (2011-BP-B-00042) and the People Program (Marie Curie Actions) of the European Union's Seventh Framework Program (FP7-PEOPLE-2012-CIG, REA grant agreement 321985). The invaluable assistance of Mrs. Montse Dominguez with the XPS measurements and analysis is greatly appreciated. F.R. thanks IGSSE (International Graduate School of Science and Engineering) and Bund der Freunde der TU München e.V. for funding. S.N. thanks CompInt (Materials Science of Complex Interfaces) of the Elite Network of Bavaria and Max Planck Society for financial support. H.K. thanks IAS (Institute for Advanced Study) of Technische Universität München, CIPSM (Center for Integrated Protein Science Munich) and King Abdulaziz University (KAU) for technical and financial support (Grant HiCi/25-3-1432).

Appendix A. Supplementary data

Supplementary data associated with this article can be found, in the online version, at http://dx.doi.org/10.1016/j.colsurfb.2014.12.057.

References

[1] R. Tejero, E. Anitua, G. Orive, Toward the biomimetic implant surface: biopolymers on titanium-based implants for bone regeneration, Prog. Polym. Sci. 39 (2014) 1406–1447, http://dx.doi.org/10.1016/j.progpolymsci.2014.01.001.
[2] M. Geetha, A.K. Singh, R. Asokamani, A.K. Gogia, Ti based biomaterials, the ultimate choice for orthopaedic implants – a review, Prog. Mater. Sci. 54 (2009) 397–425, http://dx.doi.org/10.1016/j.pmatsci.2008.06.004.
[3] K. Anselme, M. Bigerelle, Topography effects of pure titanium substrates on human osteoblast long-term adhesion, Acta Biomater. 1 (2005) 211–222, http://dx.doi.org/10.1016/j.actbio.2004.11.009.
[4] A. Wennerberg, T. Albrektsson, Effects of titanium surface topography on bone integration: a systematic review, Clin. Oral Implants Res. 20 (Suppl. 4) (2009) 172–184, http://dx.doi.org/10.1111/j.1600-0501.2009.01775.x.
[5] M. Nikkhah, F. Edalat, S. Manoucheri, A. Khademhosseini, Engineering microscale topographies to control the cell–substrate interface, Biomaterials 33 (2012) 5230–5246, http://dx.doi.org/10.1016/j.biomaterials.2012.03.079.
[6] H. Kim, F. Miyaji, T. Kokubo, T. Nakamura, Preparation of bioactive Ti and its alloys via simple chemical surface treatment, J. Biomed. Mater. Res. 32 (1996) 409–417, http://onlinelibrary.wiley.com/doi/10.1002/(SICI)1097-4636(199611)32:3%3C409::AID-JBM14%3E3.0.CO;2-B/full
[7] T. Kokubo, H.M. Kim, M. Kawashita, T. Nakamura, Bioactive metals: preparation and properties, J. Mater. Sci. Mater. Med. 15 (2004) 99–107, http://www.ncbi.nlm.nih.gov/pubmed/15330042
[8] A. Shekaran, A.J. García, Extracellular matrix-mimetic adhesive biomaterials for bone repair, J. Biomed. Mater. Res. A 96 (2011) 261–272, http://dx.doi.org/10.1002/jbm.a.32979.
[9] Y. Hirano, D.J. Mooney, Peptide and protein presenting materials for tissue engineering, Adv. Mater. 16 (2004) 17–25, http://dx.doi.org/10.1002/adma.200300383.
[10] R.O. Hynes, Integrins: bidirectional, allosteric signaling machines, Cell 110 (2002) 673–687, http://www.ncbi.nlm.nih.gov/pubmed/12297042
[11] S.J. Shattil, C. Kim, M.H. Ginsberg, The final steps of integrin activation: the end game, Nat. Rev. Mol. Cell Biol. 11 (2010) 288–300, http://dx.doi.org/10.1038/nrm2871.
[12] L.-H. Chiu, W.-F.T. Lai, S.-F. Chang, C.-C. Wong, C.-Y. Fan, C.-L. Fang, et al., The effect of type II collagen on MSC osteogenic differentiation and bone defect repair, Biomaterials 35 (2014) 2680–2691, http://dx.doi.org/10.1016/j.biomaterials.2013.12.005.
[13] I.L. Kim, S. Khetan, B.M. Baker, C.S. Chen, J.A. Burdick, Fibrous hyaluronic acid hydrogels that direct MSC chondrogenesis through mechanical and adhesive cues, Biomaterials 34 (2013) 5571–5580, http://dx.doi.org/10.1016/j.biomaterials.2013.04.004.
[14] U. Hersel, C. Dahmen, H. Kessler, RGD modified polymers: biomaterials for stimulated cell adhesion and beyond, Biomaterials 24 (2003) 4385–4415, http://dx.doi.org/10.1016/S0142-9612(03)00343-0.
[15] D.S.W. Benoit, K.S. Anseth, The effect on osteoblast function of colocalized RGD and PHSRN epitopes on PEG surfaces, Biomaterials 26 (2005) 5209–5220, http://dx.doi.org/10.1016/j.biomaterials.2005.01.045.
[16] C. Mas-Moruno, R. Fraioli, F. Albericio, J.M. Manero, F.J. Gil, Novel peptide-based platform for the dual presentation of biologically active peptide motifs on biomaterials, ACS Appl. Mater. Interfaces 6 (2014) 6525–6536, http://dx.doi.org/10.1021/am5001213.
[17] X. Chen, P. Sevilla, C. Aparicio, Surface biofunctionalization by covalent co-immobilization of oligopeptides, Colloids Surf. B: Biointerfaces 107C (2013) 189–197, http://dx.doi.org/10.1016/j.colsurfb.2013.02.005.
[18] M. Dettin, M. Conconi, R. Gambaretto, A. Pasquato, M. Folin, C. Di Bello, et al., Novel osteoblast-adhesive peptides for dental/orthopedic biomaterials, J. Biomed. Mater. Res. 60 (2002) 466–471, http://dx.doi.org/10.1002/jbm.10066.
[19] M. Dettin, A. Bagno, R. Gambaretto, G. Iucci, M.T. Conconi, N. Tuccitto, et al., Covalent surface modification of titanium oxide with different adhesive peptides: surface characterization and osteoblast-like cell adhesion, J. Biomed. Mater. Res. A 90 (2009) 35–45, http://dx.doi.org/10.1002/jbm.a.32064.
[20] J. Auernheimer, D. Zukowski, C. Dahmen, M. Kantlehner, A. Enderle, S.L. Goodman, et al., Titanium implant materials with improved biocompatibility through coating with phosphonate-anchored cyclic RGD peptides, Chembiochem 6 (2005) 2034–2040, http://dx.doi.org/10.1002/cbic.200500031.
[21] S. Hsiong, T. Boontheekul, N. Huebsch, D.J. Mooney, Cyclic arginine–glycine–aspartate peptides enhance three-dimensional stem cell osteogenic differentiation, Tissue Eng. A 15 (2009) 263–272, http://online.liebertpub.com/doi/abs/10.1089/ten.tea.2007.0411
[22] K.A. Kilian, M. Mrksich, Directing stem cell fate by controlling the affinity and density of ligand–receptor interactions at the biomaterials interface, Angew. Chem. Int. Ed. Engl. 124 (2012) 4975–4979, http://dx.doi.org/10.1002/ange.201108746.
[23] C. Mas-Moruno, P.M. Dorfner, F. Manzenrieder, S. Neubauer, U. Reuning, R. Burgkart, et al., Behavior of primary human osteoblasts on trimmed and sand-blasted Ti6Al4V surfaces functionalized with integrin αvβ3-selective cyclic RGD peptides, J. Biomed. Mater. Res. A 101 (2013) 87–97, http://dx.doi.org/10.1002/jbm.a.34303.
[24] T.A. Petrie, J.R. Capadona, C.D. Reyes, A.J. García, Integrin specificity and enhanced cellular activities associated with surfaces presenting a recombinant fibronectin fragment compared to RGD supports, Biomaterials 27 (2006) 5459–5470, http://dx.doi.org/10.1016/j.biomaterials.2006.06.027.
[25] T.A. Petrie, J.E. Raynor, C.D. Reyes, K.L. Burns, D.M. Collard, A.J. García, The effect of integrin-specific bioactive coatings on tissue healing and implant osseointegration, Biomaterials 29 (2008) 2849–2857, http://dx.doi.org/10.1016/j.biomaterials.2008.03.036.
[26] D.F. Williams, The role of short synthetic adhesion peptides in regenerative medicine; the debate, Biomaterials 32 (2011) 4195–4197, http://dx.doi.org/10.1016/j.biomaterials.2011.02.025.
[27] J. Sun, D. Wei, Y. Zhu, M. Zhong, Y. Zuo, H. Fan, et al., A spatial patternable macroporous hydrogel with cell-affinity domains to enhance cell spreading and differentiation, Biomaterials 35 (2014) 4759–4768, http://dx.doi.org/10.1016/j.biomaterials.2014.02.041.
[28] A. Rezania, K.E. Healy, Biomimetic peptide surfaces that regulate adhesion, spreading, cytoskeletal organization, and mineralization of the matrix deposited by osteoblast-like cells, Biotechnol. Prog. 15 (1999) 19–32, http://dx.doi.org/10.1021/bp980083b.
[29] H. Schliephake, D. Scharnweber, Chemical and biological functionalization of titanium for dental implants, J. Mater. Chem. 18 (2008) 2404–2414, http://dx.doi.org/10.1039/b715355b.
[30] J. Collier, T. Segura, Evolving the use of peptides as components of biomaterials, Biomaterials 32 (2011) 4198–4204, http://dx.doi.org/10.1016/j.biomaterials.2011.02.030.
[31] J. Marchand-Brynaert, E. Detrait, O. Noiset, T. Boxus, Y.J. Schneider, C. Remacle, Biological evaluation of RGD peptidomimetics, designed for the covalent derivatization of cell culture substrata, as potential promotors of cellular adhesion, Biomaterials 20 (1999) 1773–1782, http://www.ncbi.nlm.nih.gov/pubmed/10509187
[32] C. Dahmen, J. Auernheimer, A. Meyer, A. Enderle, S.L. Goodman, H. Kessler, Improving implant materials by coating with nonpeptidic, highly specific integrin ligands, Angew. Chem. Int. Ed. Engl. 43 (2004) 6649–6652, http://dx.doi.org/10.1002/anie.200460770.
[33] F. Rechenmacher, S. Neubauer, J. Polleux, C. Mas-Moruno, M. De Simone, E.A. Cavalcanti-Adam, et al., Functionalizing αvβ3- or α5β1-selective integrin antagonists for surface coating: a method to discriminate integrin subtypes in vitro, Angew. Chem. Int. Ed. Engl. 52 (2013) 1572–1575, http://dx.doi.org/10.1002/anie.201206370.
[34] F. Rechenmacher, S. Neubauer, C. Mas-Moruno, P.M. Dorfner, J. Polleux, J. Guasch, et al., A molecular toolkit for the functionalization of titanium-based biomaterials that selectively control integrin-mediated cell adhesion, Chemistry 19 (2013) 9218–9223, http://dx.doi.org/10.1002/chem.201301478.
[35] S. Gronthos, K. Stewart, Integrin expression and function on human osteoblast-like cells, J. Bone Miner. Res. 12 (1997) 1190–1197, http://onlinelibrary.wiley.com/doi/10.1359/jbmr.1997.12.8.1189/full
[36] L. Postiglione, G. Di Domenico, L. Ramaglia, S. Montagnani, S. Salzano, F. Di Meglio, et al., Behavior of SaOS-2 cells cultured on different titanium surfaces, J. Dent. Res. 82 (2003) 692–696, http://dx.doi.org/10.1177/154405910308200907.
[37] M.R. Morgan, A. Byron, M.J. Humphries, M.D. Bass, Giving off mixed signals – distinct functions of alpha5beta1 and alphavbeta3 integrins in regulating cell behaviour, IUBMB Life 61 (2009) 731–738, http://dx.doi.org/10.1002/iub.200.
[38] B. Geiger, J.P. Spatz, A.D. Bershadsky, Environmental sensing through focal adhesions, Nat. Rev. Mol. Cell Biol. 10 (2009) 21–33, http://dx.doi.org/10.1038/nrm2593.
[39] H.B. Schiller, M.-R. Hermann, J. Polleux, T. Vignaud, S. Zanivan, C.C. Friedel, et al., β1- and αv-class integrins cooperate to regulate myosin II during rigidity sensing of fibronectin-based microenvironments, Nat. Cell Biol. 15 (2013) 625–636, http://dx.doi.org/10.1038/ncb2747.
[40] P. Roca-Cusachs, N.C. Gauthier, A. Del Rio, M.P. Sheetz, Clustering of alpha(5)beta(1) integrins determines adhesion strength whereas

alpha(v)beta(3) and talin enable mechanotransduction, Proc. Natl. Acad. Sci. U.S.A. 106 (2009) 16245–16250, http://dx.doi.org/10.1073/pnas.0902818106.
[41] S. Rahmouni, A. Lindner, F. Rechenmacher, S. Neubauer, T.R.A. Sobahi, H. Kessler, et al., Hydrogel micropillars with integrin selective peptidomimetic functionalized nanopatterned tops: a new tool for the measurement of cell traction forces transmitted through αvβ3- or α5β1-integrins, Adv. Mater. 25 (2013) 5869–5874, http://dx.doi.org/10.1002/adma.201301338.
[42] O. Fromigué, J. Brun, C. Marty, S. Da Nascimento, P. Sonnet, P.J. Marie, Peptide-based activation of alpha5 integrin for promoting osteogenesis, J. Cell. Biochem. 113 (2012) 3029–3038, http://dx.doi.org/10.1002/jcb.24181.
[43] C.-F. Lai, S.-L. Cheng, Alphavbeta integrins play an essential role in BMP-2 induction of osteoblast differentiation, J. Bone Miner. Res. 20 (2005) 330–340, http://dx.doi.org/10.1359/JBMR.041013.
[44] S. Gronthos, P.J. Simmons, S.E. Graves, P.G. Robey, Integrin-mediated interactions between human bone marrow stromal precursor cells and the extracellular matrix, Bone 28 (2001) 174–181, http://www.ncbi.nlm.nih.gov/pubmed/11182375
[45] B.G. Keselowsky, D.M. Collard, A.J. García, Surface chemistry modulates fibronectin conformation and directs integrin binding and specificity to control cell adhesion, J. Biomed. Mater. Res. A 66 (2003) 247–259, http://dx.doi.org/10.1002/jbm.a.10537.
[46] S. Neubauer, F. Rechenmacher, R. Brimioulle, F.S. Di Leva, A. Bochen, T.R. Sobahi, et al., Pharmacophoric modifications lead to superpotent αvβ3 integrin ligands with suppressed α5β1 activity, J. Med. Chem. 57 (2014) 3410–3417, http://pubs.acs.org/doi/abs/10.1021/jm500092w
[47] Z. Zhong, S. Yin, C. Liu, Y. Zhong, W. Zhang, D. Shi, et al., Surface energy for electroluminescent polymers and indium-tin-oxide, Appl. Surf. Sci. 207 (2003) 183–189, http://dx.doi.org/10.1016/S0169-4332(02)01328-4.
[48] D.K. Owens, R.C. Wendt, Estimation of the surface free energy of polymers, J. Appl. Polym. Sci. 13 (1969) 1741–1747.
[49] J. Schindelin, I. Arganda-Carreras, E. Frise, V. Kaynig, M. Longair, T. Pietzsch, et al., Fiji: an open-source platform for biological-image analysis, Nat. Methods 9 (2012) 676–682, http://dx.doi.org/10.1038/nmeth.2019.
[50] T. Hanawa, A comprehensive review of techniques for biofunctionalization of titanium, J. Periodontal Implant Sci. 41 (2011) 263–272, http://dx.doi.org/10.5051/jpis.2011.41.6.263.
[51] Y. Han, D. Mayer, a. Offenhäusser, S. Ingebrandt, Surface activation of thin silicon oxides by wet cleaning and silanization, Thin Solid Films 510 (2006) 175–180, http://dx.doi.org/10.1016/j.tsf.2005.11.048.
[52] M. Godoy-Gallardo, C. Mas-Moruno, M.C. Fernández-Calderón, C. Pérez-Giraldo, J.M. Manero, F. Albericio, et al., Covalent immobilization of hLf1-11 peptide on a titanium surface reduces bacterial adhesion and biofilm formation, Acta Biomater. 10 (2014) 3522–3534, http://dx.doi.org/10.1016/j.actbio.2014.03.026.
[53] A. Bagno, C. Di Bello, Surface treatments and roughness properties of Ti-based biomaterials, J. Mater. Sci. Mater. Med. 15 (2004) 935–949, http://dx.doi.org/10.1023/B:JMSM.0000042679.28493.7f.
[54] S.J. Xiao, M. Textor, N.D. Spencer, M. Wieland, B. Keller, H. Sigrist, Immobilization of the cell-adhesive peptide Arg–Gly–Asp–Cys (RGDC) on titanium surfaces by covalent chemical attachment, J. Mater. Sci. Mater. Med. 8 (1997) 867–872, http://www.ncbi.nlm.nih.gov/pubmed/15348806
[55] S.-J. Xiao, M. Textor, N.D. Spencer, Covalent attachment of cell-adhesive, (Arg–Gly–Asp) – containing peptides to titanium surfaces, Langmuir 14 (1998) 5507–5516.
[56] J. Lincks, B.D. Boyan, C.R. Blanchard, C.H. Lohmann, Y. Liu, D.L. Cochran, et al., Response of MG63 osteoblast-like cells to titanium and titanium alloy is dependent on surface roughness and composition, Biomaterials 19 (1998) 2219–2232, http://www.ncbi.nlm.nih.gov/pubmed/9884063
[57] X. Lu, Z. Zhao, Y. Leng, Biomimetic calcium phosphate coatings on nitric-acid-treated titanium surfaces, Mater. Sci. Eng. C 27 (2007) 700–708, http://dx.doi.org/10.1016/j.msec.2006.06.030.
[58] S.B. Kennedy, N.R. Washburn, C.G. Simon, E.J. Amis, Combinatorial screen of the effect of surface energy on fibronectin-mediated osteoblast adhesion, spreading and proliferation, Biomaterials 27 (2006) 3817–3824, http://dx.doi.org/10.1016/j.biomaterials.2006.02.044.
[59] A. Rezania, R. Johnson, A. Lefkow, K. Healy, Bioactivation of metal oxide surfaces. 1. Surface characterization and cell response, Langmuir 15 (1999) 6931–6939, http://pubs.acs.org/doi/abs/10.1021/la990024n
[60] R. Pankov, Fibronectin at a glance, J. Cell Sci. 115 (2002) 3861–3863, http://dx.doi.org/10.1242/jcs.00059.
[61] C.J. Wilson, R.E. Clegg, D.I. Leavesley, M.J. Pearcy, Mediation of biomaterial–cell interactions by adsorbed proteins: a review, Tissue Eng. 11 (2005) 1–18, http://dx.doi.org/10.1089/ten.2005.11.1.
[62] C.H. Thomas, C.D. McFarland, M.L. Jenkins, A. Rezania, J.G. Steele, K.E. Healy, The role of vitronectin in the attachment and spatial distribution of bone-derived cells on materials with patterned surface chemistry, J. Biomed. Mater. Res. 37 (1997) 81–93, http://www.ncbi.nlm.nih.gov/pubmed/9335352
[63] A.J. Garcia, J. Takagi, D. Boettiger, Two-stage activation for alpha5beta1 integrin binding to surface-adsorbed fibronectin, J. Biol. Chem. 273 (1998) 34710–34715, http://dx.doi.org/10.1074/jbc.273.52.34710.
[64] M.C. Siebers, P.J. ter Brugge, X.F. Walboomers, J.A. Jansen, Integrins as linker proteins between osteoblasts and bone replacing materials. A critical review, Biomaterials 26 (2005) 137–146, http://dx.doi.org/10.1016/j.biomaterials.2004.02.021.
[65] G. Gronowicz, M.B. McCarthy, Response of human osteoblasts to implant materials: integrin-mediated adhesion, J. Orthop. Res. 14 (1996) 878–887, http://dx.doi.org/10.1002/jor.1100140606.
[66] B.G. Keselowsky, D.M. Collard, A.J. García, Integrin binding specificity regulates biomaterial surface chemistry effects on cell differentiation, Proc. Natl. Acad. Sci. U.S.A. 102 (2005) 5953–5957, http://dx.doi.org/10.1073/pnas.0407356102.
[67] E.H.J. Danen, P. Sonneveld, C. Brakebusch, R. Fässler, A. Sonnenberg, The fibronectin-binding integrins alpha5beta1 and alphavbeta3 differentially modulate RhoA-GTP loading, organization of cell matrix adhesions, and fibronectin fibrillogenesis, J. Cell Biol. 159 (2002) 1071–1086, http://dx.doi.org/10.1083/jcb.200205014.
[68] R. Seger, E.G. Krebs, The MAPK signaling cascade, FASEB J. 9 (1995) 726–735, http://www.fasebj.org/content/9/9/726.short
[69] E.A. Cowles, L.L. Brailey, G.A. Gronowicz, Integrin-mediated signaling regulates AP-1 transcription factors and proliferation in osteoblasts, J. Biomed. Mater. Res. 52 (2000) 725–737, http://www.ncbi.nlm.nih.gov/pubmed/11033556
[70] M.M. Martino, M. Mochizuki, D.A. Rothenfluh, S.A. Rempel, J.A. Hubbell, T.H. Barker, Controlling integrin specificity and stem cell differentiation in 2D and 3D environments through regulation of fibronectin domain stability, Biomaterials 30 (2009) 1089–1097, http://dx.doi.org/10.1016/j.biomaterials.2008.10.047.
[71] M. Kantlehner, P. Schaffner, D. Finsinger, J. Meyer, A. Jonczyk, B. Diefenbach, et al., Surface coating with cyclic RGD peptides stimulates osteoblast adhesion and proliferation as well as bone formation, Chembiochem 1 (2000) 107–114, http://www.ncbi.nlm.nih.gov/pubmed/11828404
[72] M. López-Garcia, H. Kessler, Stimulation of bone growth on implants by integrin ligands, in: M. Epple, E. Bäuerlein (Eds.), Handb. Miner, Wiley-VCH, Weinheim, Germany, 2007, pp. 109–126.
[73] C.-H. Ku, D.P. Pioletti, M. Browne, P.J. Gregson, Effect of different Ti-6Al-4V surface treatments on osteoblasts behaviour, Biomaterials 23 (2002) 1447–1454, http://www.ncbi.nlm.nih.gov/pubmed/11829440
[74] L. Shapira, A. Halabi, Behavior of two osteoblast-like cell lines cultured on machined or rough titanium surfaces, Clin. Oral Implants Res. 20 (2009) 50–55, http://dx.doi.org/10.1111/j. 1600-0501.2008.01594.x.
[75] A. Klinger, A. Tadir, A. Halabi, L. Shapira, The effect of surface processing of titanium implants on the behavior of human osteoblast-like Saos-2 cells, Clin. Implant Dent. Relat. Res. 13 (2011) 64–70, http://dx.doi.org/10.1111/j. 1708-8208.2009.00177.x.
[76] E. De Angelis, F. Ravanetti, A. Cacchioli, A. Corradi, C. Giordano, G. Candiani, et al., Attachment, proliferation and osteogenic response of osteoblast-like cells cultured on titanium treated by a novel multiphase anodic spark deposition process, J. Biomed. Mater. Res. B: Appl. Biomater. 88 (2009) 280–289, http://dx.doi.org/10.1002/jbm.b.31179.
[77] H.A. Declercq, R.M.H. Verbeeck, L.I.F.J.M. De Ridder, E.H. Schacht, M.J. Cornelissen, Calcification as an indicator of osteoinductive capacity of biomaterials in osteoblastic cell cultures, Biomaterials 26 (2005) 4964–4974, http://dx.doi.org/10.1016/j.biomaterials.2005.01.025.
[78] S.L. Cheng, C.F. Lai, S.D. Blystone, L.V. Avioli, Bone mineralization and osteoblast differentiation are negatively modulated by integrin alpha(v)beta3, J. Bone Miner. Res. 16 (2001) 277–288, http://dx.doi.org/10.1359/jbmr.2001.16.2.277.
[79] G.B. Schneider, R. Zaharias, C. Stanford, Osteoblast integrin adhesion and signaling regulate mineralization, J. Dent. Res. 80 (2001) 1540–1544, http://cat.inist.fr/?aModele=afficheN&cpsidt=13472617
[80] G. Stein, J. Lian, T. Owen, Relationship of cell growth to the regulation of tissue-specific gene expression during osteoblast differentiation, FASEB J. 4 (1990) 3111–3123, http://www.fasebj.org/content/4/13/3111.short